

Optical property measurements of 235 mm large-scale Ti:sapphire crystal

He Cao (曹鹤)^{1,3}, Zebiao Gan (甘泽彪)¹, Xiaoyan Liang (梁晓燕)^{1,*},
Lianghong Yu (於亮红)¹, Wenqi Li (李文启)^{1,3}, Zhen Guo (郭振)^{1,3}, Pei Huang (黄培)^{1,3},
Jianye Wang (王建业)^{1,3}, Min Xu (徐民)², and Yin Hang (杭寅)^{2,**}

¹State Key Laboratory of High Field Laser Physics, Shanghai Institute of Optics and Fine Mechanics, Chinese Academy of Sciences, Shanghai 201800, China

²Key Laboratory of Materials for High Power Laser, Shanghai Institute of Optics and Fine Mechanics, Chinese Academy of Sciences, Shanghai 201800, China

³University of Chinese Academy of Sciences, Chinese Academy of Sciences, Beijing 100049, China

*Corresponding author: liangxy@sioim.ac.cn; **corresponding author: yhang@sioim.ac.cn

Received March 22, 2018; accepted May 8, 2018; posted online June 25, 2018

A Ti:sapphire crystal with a diameter of 235 mm and thickness of 72 mm was grown by the heat exchange method (HEM). The absorption intensity of the crystal at 532 nm averaged at 91%. The figures of merit (FOMs) at different positions of the crystal were measured and the FOM value in the central region was found to reach 90. The transmittance laser beam was intact with no obvious distortions and had only a small deformation compared with the incident laser beam. A small-signal amplification experiment was performed on the Ti:sapphire crystal and a gain of more than 6 times was achieved with a pump energy density of 1.98 J/cm². These tests indicate that the 235 mm Ti:sapphire crystal has excellent optical qualities and will further improve the energy output of a 10 PW laser system.

OCIS codes: 140.3280, 140.3590, 140.5560, 140.7090.

doi: 10.3788/COL201816.071401.

The emergence of ultra-intense and ultrashort laser systems makes it possible to attain the ultrahigh energy density extreme conditions in the laboratory that are otherwise found only in the interior of a star or the edge of a black hole. It has largely promoted the development of a number of basic and frontier interdisciplinary subjects including laser science, attosecond optics, and plasma physics. Ultra-intense ultrashort laser applications have made some progress in driving the wake field electron acceleration, achieving controlled thermonuclear fusion and detection of ultra-fast processes^[1-5].

Chirped pulse amplification (CPA) technology, proposed in 1985, accelerated the development of ultra-intense and ultrashort laser systems^[6]. The core device of ultra-intense and ultrashort laser systems is a laser crystal that produces femtosecond ultrashort pulses. Ti:sapphire crystals have a wide gain bandwidth (660–1200 nm), excellent physical and chemical properties (thermal conductivity 0.43 W/cm² and melting point 2050°C), and their shortest pulse width is 3.3 fs by theoretical calculation after the wide emission spectrum is compressed. Hence, Ti:sapphire crystals are currently recognized as the ideal femtosecond ultrafast laser crystal^[7].

Large-scale Ti:sapphire crystals are required to meet the requirements for higher-power laser systems. The Kyropoulos method (KY)^[8], the heat exchange method^[9] (HEM), the temperature gradient method^[10] (TGT), and horizontal directional solidification^[11] (HDS) are the principal methods used to grow large-scale Ti:sapphire crystals. The HEM is the preferred method for its

numerous advantages over other methods^[12] including independently controlling the temperature gradient of the melt and the crystal, a stable growth interface, reducing conditions that inhibit the formation of Ti⁴⁺ ions, and post growth *in situ* isothermal annealing.

An energy of 202.8 J and a corresponding peak power of 5.4 PW were achieved based on CPA technology and a new temporal multi-pulse pump scheme^[13] by the Shanghai Super-intense Ultrafast Laser Facility (SULF) using a Ti:sapphire crystal of diameter 150 mm; these were the highest energy and peak-power outputs ever reported for a petawatt femtosecond-class laser system^[14]. Many countries plan to construct an ultra-intense and ultrashort laser facility such as France's APOLLON 10 PW facility^[15] and England's Vulcan project^[16] for 10 PW laser pulse output. SULF also aims to use a 72 mm thick Ti:sapphire crystal wafer with 235 mm in diameter as the final amplifier based on a 5 PW laser system to support 10 PW output.

For this study, a Ti:sapphire crystal wafer with 235 mm in diameter and 72 mm in thickness grown by the HEM was acquired from the Shanghai Institute of Optics and Fine Mechanics, Chinese Academy of Sciences. To the best of our knowledge, this is the largest Ti:sapphire crystal ever reported for a petawatt femtosecond-class laser system. Optical property measurements of the Ti:sapphire crystal were carried out.

The Ti:sapphire crystal is a uniaxial crystal. Its absorption of the pump laser is dependent on the polarization direction of the pump laser. When the polarization

direction of the pump laser is parallel to the c axis of the crystal (π polarization), the absorption of the pump laser beam by the Ti:sapphire crystal is the strongest. When the polarization direction of the pump laser is perpendicular to the c axis of the crystal (σ polarization), the absorption of the pump laser by the Ti:sapphire crystal is the weakest. We aligned the c axis of the Ti:sapphire crystal parallel with the polarization direction of the pump laser during its installation on the crystal cartridge, thus achieving the strongest absorption condition.

We measured the transmittance and the corresponding absorption coefficient at different positions along the horizontal and vertical diameter directions. The absorption intensity of the Ti:sapphire crystal for a 532 nm pump laser and the characteristics of the distribution of Ti^{3+} ions can be obtained from these data. We started with the center of the Ti:sapphire crystal and considered points at a distance of every 10 mm in the direction of the horizontal and the vertical diameter, respectively. These positions were marked as $-11, -10, -9, \dots, 0, 1, 2, 3, \dots, 11$; the maximum absorption coefficient at these points was measured with a test laser beam of 10 mm diameter and 532 nm wavelength. The measurement results are shown in Fig. 1.

Two curves of the absorption coefficient and transmittance are shown in Fig. 1. It can be clearly seen that the variation trend of the horizontal and the vertical diameter directions is basically the same. In terms of transmittance, the center point has the highest transmittance of 8.46% from which the transmittance decreases gradually on either side; the variation trend presents a parabolic curve. Marginal transmittance is only about 0.3%, indicating that the concentration of Ti^{3+} ions at the center of the Ti:sapphire crystal is low while it is high on the edges. The test result conforms to the characteristics of the Ti^{3+} ion concentration distribution of the Ti:sapphire crystal grown by the HEM. The solid-liquid interface is generally controlled as a convex interface during the growth of Ti:sapphire crystals by the HEM. The segregation coefficient of Ti^{3+} ions in the crystal is only 0.16 (far less than 1). These factors cause the concentration of Ti^{3+} ions at the top of the crystal to be higher than at the bottom of the crystal, and the edge concentration to be higher than the central concentration.

The figure of merit (FOM) of the Ti:sapphire crystal is defined as the ratio of the absorption coefficient for the absorption wavelength to the absorption coefficient for the emission wavelength. The larger the value of the FOM, the higher the optical gain of the crystal^[17]. Hence, a Ti:sapphire crystal with a high FOM value is desired. The absorption coefficient of the Ti:sapphire crystal is characterized by the formula

$$a = \frac{\ln T}{L}, \quad (1)$$

where a , L , and T are the absorption coefficient, thickness, and transmittance of the Ti:sapphire crystal^[18], respectively. Hence, we focus on measuring the transmittance

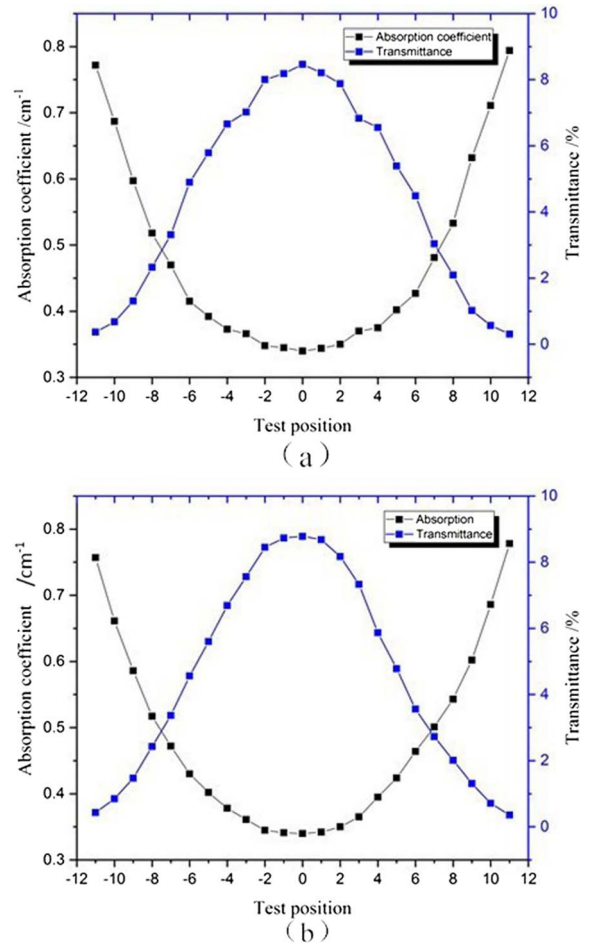


Fig. 1. Absorption coefficient and transmittance at different positions of the Ti:sapphire crystal for (a) the horizontal diameter direction and (b) the vertical diameter direction.

for an 800 nm wavelength laser and then the absorption coefficient at 800 nm is calculated. A double laser beam light path system was used in the measurements to avoid any measurement error caused by the energy fluctuation of the laser source. The absorption coefficient was measured at five different positions of the Ti:sapphire crystal.

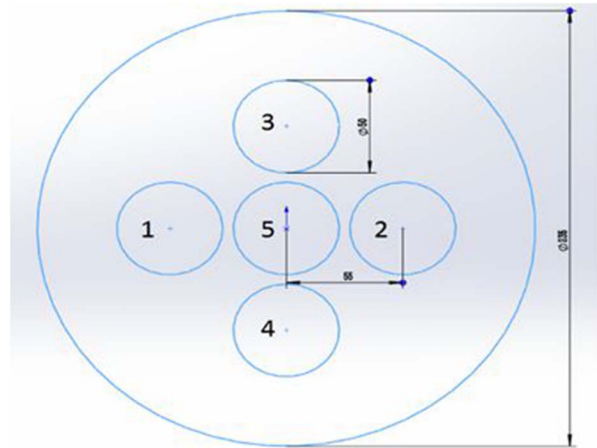


Fig. 2. Test positions.

Table 1. FOM of the Ti:Sapphire Crystal

Test Position	1	2	3	4	5
Transmittance of 532 nm laser/%	4.99	4.67	3.81	4.61	8.02
Absorption coefficient of 532 nm laser/cm ⁻¹	0.4129	0.4222	0.4500	0.4239	0.3476
Transmittance of 800 nm laser/%	96.60	96.84	95.89	95.66	97.26
Absorption coefficient of 800 nm laser/cm ⁻¹	0.0048	0.0045	0.0058	0.0062	0.0039
FOM (a_{532}/a_{800})	86.0	93.8	77.6	68.4	89.1

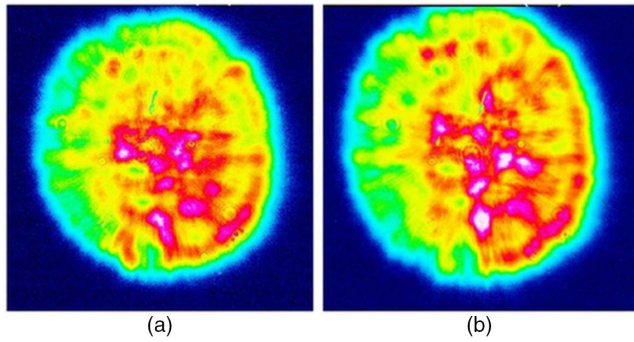


Fig. 3. (a) 1 Hz static incident laser beam and (b) 1 Hz transmittance laser beam.

The diameter of the test laser beam was 50 mm; the test areas are shown in Fig. 2. Table 1 shows the transmission ratio, absorption coefficient, and corresponding FOM values of the test positions.

As can be seen from the table, the FOM value of position 4 of the Ti:sapphire crystal is smaller than the values at other parts. The reason may be that a relatively large number of Ti⁴⁺ ions are gathered in the position 4 part of the Ti:sapphire crystal. There is direct correlation between Ti⁴⁺ ions and residual absorption near 800 nm, resulting in a relatively strong absorption of 800 nm light

and a lower FOM value^[19]. The FOM value near the center of the Ti:sapphire crystal reached 89.1 and it was greater than 77 in all the other regions except for position 4, indicating the high quality of the Ti:sapphire crystal.

The incident laser beam and the transmittance laser beam of the broadband seed pulse, which has a diameter of 180 mm and a central wavelength at 800 nm, were detected by a CCD digital camera and are shown in Fig. 3.

It can be seen from Fig. 3 that the shape of the transmittance laser beam is intact; there is no obvious distortion. There is only a small deformation between the incident laser beam and the transmittance laser beam, indicating a high intrinsic quality of Ti:sapphire crystal without defects like precipitate phase, micropores, and secondary phase inclusions.

We used a set of homemade Nd:glass laser systems to conduct the single-pass amplification experiment for small-signal seeding energy of the Ti:sapphire crystal. The overall layout of the experimental setup is presented in Fig. 4. The Ti:sapphire crystal is double-end pumped. The pump laser beam has a diameter of about 17 mm and its energy is 4.5 J, so the pump energy density is 1.98 J/cm². The broadband seed pulse with a central wavelength at 800 nm has a 5 mJ energy output and a beam diameter of 13 mm. We started with the center point of the Ti:sapphire crystal and considered points every 20 mm along the vertical and horizontal diameter directions.

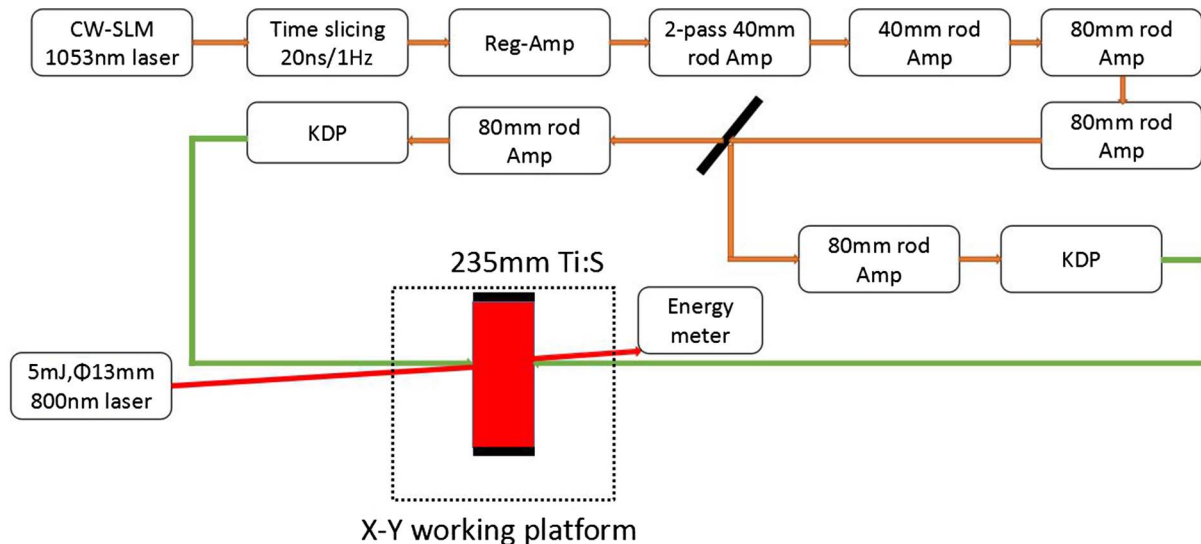


Fig. 4. Ti:sapphire crystal small-signal amplification experimental optical path.

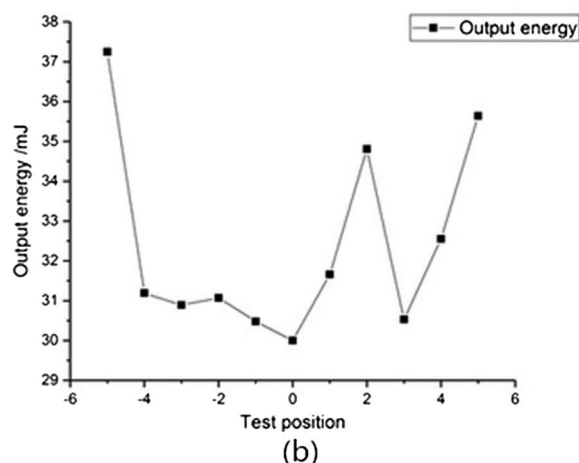
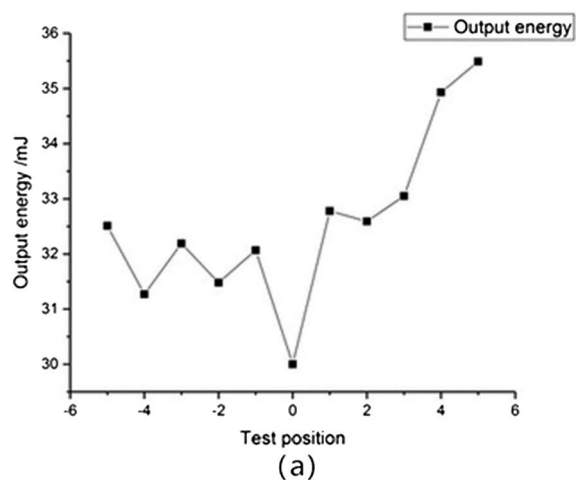


Fig. 5. Output energy value of the small-signal amplification experiment of the Ti:sapphire crystal for (a) the horizontal diameter direction and (b) the vertical diameter direction.

The locations were labeled as $-5, -4, \dots, 0, \dots, 4, 5$. The values of the small-signal gain at these locations were tested. The measurement results are presented in Fig. 5.

It can be seen from Fig. 5 that the small-signal gain values for single-pass amplification of most of the test locations are approximately in the range of 6–7 with a pump energy density of 1.98 J/cm^2 . The small-signal gain of the test location near the edge of the Ti:sapphire crystal is higher than that at the other test locations, proving the edge concentration of Ti^{3+} ions to be higher than the central concentration again.

In conclusion, a Ti:sapphire crystal wafer with 235 mm in diameter and 72 mm in thickness grown by the HEM was acquired from the Shanghai Institute of Optics and Fine Mechanics. The absorption intensity for the laser with wavelength 532 nm was found to be more than 91% and the edge absorption was higher than the central absorption, which conforms to the characteristics of the Ti^{3+} ion concentration distribution of the Ti:sapphire crystal grown by

the HEM. The FOM value for the central area of the Ti:sapphire crystal was as high as 90. The transmittance laser beam was complete with no obvious distortion. The small-signal gain values at different positions of the Ti:sapphire crystal were more than 6 with a pump energy density of 1.98 J/cm^2 . These tests indicate that the 235 mm Ti:sapphire crystal has high optical qualities and will further improve the energy output of 10 PW laser system.

This work was supported by the National Natural Science Foundation of China (Nos. 61775223 and 51502321), the Strategic Priority Research Program of Chinese Academy of Sciences (No. XDB1603), and the Shanghai Scientific Research Project (Nos. 16JC1420600 and 16DZ0503900).

References

1. R. X. Li, Y. X. Leng, and Z. Z. Xu, *Phys.* **44**, 509 (2015).
2. T. Miyakoshi, K. A. Tanaka, A. E. Dangor, Y. Toyama, and Y. Kitagawa, *Nature* **412**, 798 (2001).
3. A. Baltuska, T. Udem, M. Uiberacker, V. S. Yakovlev, and R. Holzwarth, *Nature* **421**, 611 (2003).
4. A. H. Zewail, *J. Phys. Chem. A* **104**, 5660 (2000).
5. R. L. Kodama, *Nature* **418**, 933 (2002).
6. D. Strickland and G. Mourou, *Opt. Commun.* **56**, 219 (1985).
7. J. L. Si, J. Xu, G. J. Zhao, G. Q. Zhou, H. J. Li, J. Y. Wang, and P. Z. Deng, *Chin. J. Lasers* **31**, 381 (2004).
8. C. Stelian, G. Alombert-Goget, G. Sen, N. Barthalay, and K. Lebbouet, *Opt. Mater.* **69**, 73 (2017).
9. D. B. Joyce and F. Schmid, *J. Cryst. Growth* **312**, 1138 (2009).
10. Y. Z. Zhou, "The TGT growth devices for high-temperature crystals," China Patent 85100534.9 (Nov. 24, 1988).
11. S. V. Nizhankovskiy, Y. A. Dan'ko, E. V. Krivonosov, and V. M. Puzikoval, *Inorg. Mater.* **46**, 35 (2010).
12. K. J. Ning, Y. C. Liu, J. Ma, L. H. Lian, X. Y. Liang, D. Y. Tang, R. X. Li, and Y. Hang, *Cryst. Eng. Com.* **17**, 2801 (2015).
13. Z. B. Gan, X. Y. Liang, L. H. Yu, J. Q. Hong, M. Xu, Y. Hang, and R. X. Li, *Chin. Opt. Lett.* **15**, 091401 (2017).
14. Z. B. Gan, L. H. Yu, S. Li, C. Wang, X. Y. Liang, Y. Q. Liu, W. Q. Li, Z. Guo, Z. T. Fan, X. L. Yuan, L. Xu, Z. Z. Liu, Y. Xu, J. Lun, H. H. Lu, D. J. Yin, Y. X. Leng, R. X. Li, and Z. Z. Xu, *Opt. Express* **25**, 5169 (2017).
15. D. N. Papadopoulos, J. P. Zou, C. Le Blanc, G. Cheriaux, P. Georges, F. Druon, G. Mennerat, P. Ramirez, L. Martin, A. Freneaux, A. Beluze, N. Lebas, P. Monot, F. Mathieu, and P. Audebert, *High Power Laser Sci. Eng.* **4**, e34 (2016).
16. C. Hernandez-Gomez, S. P. Blake, O. Chekhlov, R. J. Clarke, A. M. Dunne, M. Galimberti, S. Hancock, R. Heathcote, P. Holligan, A. Lyachev, P. Matousek, I. O. Musgrave, D. Neely, P. A. Norreys, I. Ross, Y. Tang, T. B. Winstone, and B. E. Wyborn, *J. Phys.* **244**, 032006 (2010).
17. P. Yan, L. Su, B. Y. Ding, Y. Yang, and G. W. Zhang, *Opto-Electron. Eng.* **24**, 46 (1997).
18. X. C. Zhang, J. L. Si, M. Xu, X. Y. Liang, and Y. X. Chu, *Chin. J. Lasers* **41**, 0506001 (2014).
19. R. L. Aggarwal, A. Sanchez, and M. M. Stuppi, *J. Quantum Electron.* **24**, 1003 (1988).